

# Study of the decomposition of aqueous citratoperoxo-Ti(IV)-gel precursors for titania by means of TGA-MS and FTIR

I. Truijen<sup>a</sup>, A. Hardy<sup>a</sup>, M.K. Van Bael<sup>a,b</sup>, H. Van den Rul<sup>a,b</sup>, J. Mullens<sup>a,\*</sup>

<sup>a</sup> Hasselt University, Institute for Materials Research, Laboratory of Inorganic and Physical Chemistry, Agoralaan-building D, B-3590 Diepenbeek, Belgium

<sup>b</sup> IMEC vzw, Division IMOMECE, Agoralaan-building D, B-3590 Diepenbeek, Belgium

Received 18 December 2006; received in revised form 23 January 2007; accepted 26 January 2007

Available online 3 February 2007

## Abstract

An aqueous solution–gel route is developed for the preparation of TiO<sub>2</sub>. In this report, we study an aqueous citratoperoxo-Ti(IV)-precursor at pH 2.0, which is compatible with polyvinyl alcohol (PVA) and therefore can be applied for the preparation of a thick mesoporous TiO<sub>2</sub> film.

With regard to deposition of films, it is important to gain insight in the behaviour of the precursor during thermal treatment. Therefore, the thermal decomposition mechanism of a citratoperoxo-Ti(IV)-gel and a PVA modified citratoperoxo-Ti(IV)-gel is studied. Weight losses and evolved gasses are characterized by TGA-MS (5 °C min<sup>-1</sup>), while gel structure and changes in the solid upon heating are studied by means of FTIR. For both gels, decomposition in dry air can be divided into five regions. After drying of the samples in the first region (~100 °C), decomposition of the organic matter not coordinated to the metal ions occurs (~200 °C). The third region (~310 °C) involves the decomposition of citrato ligands. Finally, the residual organic matter is combusted in the last two regions. Only in dry air it is possible to fully remove the organic matrix in both gels at temperatures below 600 °C.

It is also proven that the citratoperoxo-Ti(IV)-complexes, seen at pH 7.0, exist in the precursor gel already at pH 2.0.

© 2007 Elsevier B.V. All rights reserved.

**Keywords:** Aqueous solution–gel method; PVA; Thermal decomposition; TiO<sub>2</sub>; TGA-EGA; FTIR

## 1. Introduction

Titanium dioxide (TiO<sub>2</sub>) has attracted great scientific and technological attention because of its versatile chemical and physical properties. It is a biocompatible, chemically inert semiconductor which shows a high photostability, is readily available and cheap. Due to these properties, the material is useful in several applications such as photovoltaic cells [1–4], gas sensors [5] and photocatalysts [1,6–9]. Nanocrystalline titania has been synthesized either as a powder [10,11] or as a thin [12–14] or thick [15] film by various methods such as sputter techniques [16–21], chemical vapour deposition (CVD) [22–25] and sol–gel synthesis [10–15,26–28]. To prepare mesoporous TiO<sub>2</sub>, ionic and neutral surfactants have been successfully employed as tem-

plates during sol–gel synthesis [27,29]. Also block copolymers have been used to direct formation of mesoporous titania [30]. In addition, non-surfactant organic compounds have been used as pore formers such as polyethyleneglycol [31,32], hydroxypropylcellulose [26], diolates [33] and cyclodextrines [34].

In our laboratory, several (multi-)metal oxides have been synthesized successfully via sol(ution)–gel routes, alcoholic as well as aqueous [35–40]. The aqueous route shows the same advantages as its conventional alcoholic counterpart but it has the surplus of being economically and ecologically friendly. Furthermore, no special precautions to protect the starting products and precursor solutions from air or humidity have to be taken. This method has turned out to be an interesting approach for the synthesis of several electroceramic materials, both powders and thin films [36–40].

In this study, an aqueous citratoperoxo solution–gel route is applied for the preparation of mesoporous TiO<sub>2</sub>. In order to obtain a highly viscous Ti(IV)-precursor paste, the Ti(IV)-precursor solution is modified by the addition of polyvinyl alcohol (PVA). The latter acts as a thickener and pore former

\* Corresponding author. Tel.: +32 11 26 83 08; fax: +32 11 26 83 01.

E-mail addresses: [ine.truijen@uhasselt.be](mailto:ine.truijen@uhasselt.be) (I. Truijen), [an.hardy@uhasselt.be](mailto:an.hardy@uhasselt.be) (A. Hardy), [marlies.vanbael@uhasselt.be](mailto:marlies.vanbael@uhasselt.be) (M.K. Van Bael), [heidi.vandenrul@uhasselt.be](mailto:heidi.vandenrul@uhasselt.be) (H. Van den Rul), [jules.mullens@uhasselt.be](mailto:jules.mullens@uhasselt.be) (J. Mullens).

[15]. In earlier work we have seen that the solubility of PVA in the citratoperoxo-Ti(IV)-precursor solution is dependent on the pH and an acidic precursor pH (pH = 2) is required [15]. The resulting precursor paste is tapecasted to obtain a film.

In previous research [41] an aqueous citratoperoxo-Ti(IV)-precursor at neutral pH (pH = 7.0) is described. It is shown that in this precursor  $\text{Ti}^{4+}$  ions are encapsulated in a citratoperoxo-Ti(IV)-complex. From a citratoperoxo-Ti(IV)-precursor solution at pH = 7.0 a crystalline complex was obtained [42]. Its structure was studied by means of XRD and it was shown to be identical to  $(\text{NH}_4)_8[\text{Ti}_4(\text{C}_6\text{H}_4\text{O}_7)_4(\text{O}_2)_4] \cdot 8\text{H}_2\text{O}$ , which is described by Kakihana et al. [43].

Here, we want to examine if, even at a low pH (pH = 2.0),  $\text{Ti}^{4+}$  ions in the precursor gel form part of a citratoperoxo-complex. The  $\text{pK}_a$  values of citric acid are 3.13, 4.76 and 6.40. Consequently, none of the acid functions is expected to be deprotonated at pH = 2.0. However, the dissociation equilibrium of citric acid can possibly be shifted to the right (lower pH values) by the complexation equilibrium between the deprotonated citric acid and  $\text{Ti}^{4+}$ .

In this study, we also want to evaluate the influence of the pH and the presence of PVA on the thermal decomposition pathway of the precursor solution. The desired oxide phase can be obtained by an appropriate heat treatment of the amorphous precursor gel. In order to optimize this heat treatment, insight into the precursor's behaviour during thermal decomposition is of great importance. Therefore, the thermal decomposition of a citratoperoxo-Ti(IV)-gel and a PVA modified citratoperoxo-Ti(IV)-gel, both prepared at pH 2.0, is studied by thermoanalytical techniques.

## 2. Experimental

### 2.1. Materials and reagents

For gel synthesis the following reagents are used: Ti(IV)-isopropoxide ( $\text{Ti}(\text{iOPr})_4$ , 98+%, Acros), citric acid ( $\text{C}_6\text{H}_8\text{O}_7$ , 99%, Aldrich), hydrogen peroxide ( $\text{H}_2\text{O}_2$ , 35 wt.% in  $\text{H}_2\text{O}$ , p.a., stabilized, Acros) and ammonia ( $\text{NH}_3$ , 32% in  $\text{H}_2\text{O}$ , extra pure, Merck). Polyvinyl alcohol (Acros, MW 88,000, 88% hydrolyzed) is used as a thickener.

### 2.2. Aqueous solution–gel synthesis

Citratoperoxo-Ti(IV)-precursor solutions with a 0.8 M Ti(IV)-concentration are prepared in a similar way as described elsewhere [12,36,38,40]. Hydrolysis of Ti(IV)-isopropoxide in  $\text{H}_2\text{O}$  leads to the precipitation of a hydroxide to which an excess of citric acid and  $\text{H}_2\text{O}_2$  is added in a molar ratio versus Ti(IV) of respectively 2:1 and 1.2:1. The pH of the resulting 0.8 M citratoperoxo-Ti(IV)-precursor solution (pH = 0.3) is increased by the addition of ammonia up to pH = 2.0. Clear, red coloured solutions are obtained.

The viscosity of the Ti(IV)-precursor solution is increased by the addition of an aqueous solution of polyvinyl alcohol. In a separate container a PVA solution (15 wt.% in water) is prepared by dissolving 6 g PVA in 34 g distilled water, followed by contin-

uous stirring at 70 °C during 10 h. The resulting, clear, polymer solution is added to the citratoperoxo-Ti-precursor solution in a 1:1 weight ratio. In this way, a highly viscous orange precursor solution, containing 7.5 wt.% PVA, is obtained [15].

Gelation and drying of the gels is carried out on a Petri dish, in a furnace at 60 °C under flowing air, during 4 h. Upon solvent evaporation, both the unmodified and modified citratoperoxo-Ti(IV)-precursor solutions convert into amorphous gels. The resulting gels are ground and used for further investigation.

### 2.3. Characterization techniques

The thermal decomposition pathways of the Ti(IV)-precursor gels are examined by means of thermogravimetric analysis (TGA) (TA Instruments TGA 951-2000) on-line coupled with a quadrupole mass spectrometer (MS, Thermolab VG Fisons), using a flexible heated silica lined steel capillary and a molecular leak. This technique allows the analysis of the evolved gases during heating (TGA-EGA). The evolving gas molecules are fragmented during ionization. In order to avoid fragmentation of  $\text{H}_2\text{O}$  into  $\text{OH}^+$ , which would interfere with the signal of  $\text{NH}_3^+$  at  $m/z$  17, all measurements are carried out at an ionization energy of 20 eV instead of 70 eV, which is usually applied [44]. Scans are performed in the range between  $m/z$  = 10 and 110, because the most important ions are expected to be situated here.

All TGA experiments are performed using a heating rate of 5 °C  $\text{min}^{-1}$  in an atmosphere of 100  $\text{ml min}^{-1}$  synthetic dry air (mixture of 20%  $\text{O}_2$  and 80%  $\text{N}_2$ ) or pure  $\text{N}_2$ .

Sample composition of both gels at room temperature and changes occurring in the solid phase during thermal decomposition of the PVA modified citratoperoxo-Ti(IV)-gel are studied by Fourier transform infrared spectroscopy (FTIR, Bruker IFS 66, resolution: 4  $\text{cm}^{-1}$ ). The modified gel is heated in a TGA furnace to specified temperatures and quenched to room temperature. The quenched powders are mixed with KBr (0.5 wt.%) and compressed into pellets. Afterwards FTIR spectra of the pellets, prepared in this way, are recorded at room temperature in a wavenumber region of 400 to 4000  $\text{cm}^{-1}$ .

XRD spectra are recorded on a Siemens D-5000 diffractometer with  $\text{Cu K}\alpha 1$  radiation.

## 3. Results and discussion

### 3.1. Citratoperoxo-Ti(IV)-precursor gel

#### 3.1.1. Thermal decomposition

In order to be able to assign certain mass fragments detected with TGA-MS, a reference TGA-MS spectrum of citric acid is recorded (Fig. 1). A selection of typical mass fragments is shown as a function of temperature in Fig. 1b. The most important mass fragments are listed in Table 1.

The TGA and DTG data of the citratoperoxo-Ti(IV)-precursor gel, measured at a heating rate of 5 °C  $\text{min}^{-1}$  in dry air and inert atmosphere ( $\text{N}_2$ ) are shown in respectively Fig. 2a and b.

Decomposition of the citratoperoxo-Ti(IV)-precursor gel without PVA in dry air occurs in five regions centered at 100,

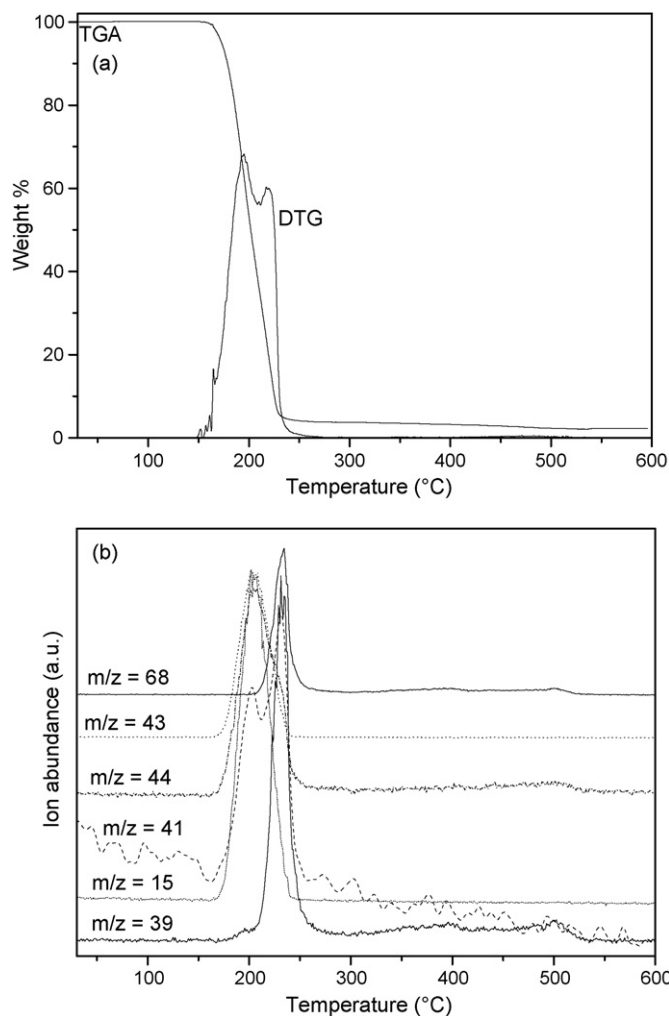


Fig. 1. (a) TGA/DTG and (b) TGA-MS for reference citric acid (25 mg,  $C_6H_8O_7$ , 99%, Aldrich) in dynamic air ( $5^\circ C\ min^{-1}$ ).

Table 1

Occurrence of mass fragments in TGA-MS of the reference citric acid ( $C_6H_8O_7$ , 99%, Aldrich)

$m/z$	Fragment(s)
15	$CH_3^+$
18	$H_2O^+$
39	$C_3H_3^+$
40	$C_3H_4^+$
41	$^{13}C_3H_4^+$
42	$C_2H_2O^+$
43	$C_2H_3O^+$
44	$CO_2^+$
45	$COOH^+$ ; $^{13}COO^+$
46	$^{13}COOH^+$
68	$C_4H_4O^+$

200, 310, 460 and  $520^\circ C$  (Fig. 2a). The second region comprises two maxima indicating that at this temperature overlapping processes are certainly taking place. The last two regions are not seen in inert atmosphere and the third region does not occur exactly at the same temperature indicating the influence of atmospheric  $O_2$  in these regions (Fig. 2b).

The gases evolved during the five regions of the citratoperoxo-Ti(IV)-gel decomposition are analyzed by MS. The assignment of the most important mass fragments is listed in Table 2. A selection of some ion abundances as a function of temperature is shown in Fig. 3. The assignment of the mass fragments detected in TGA-MS is based on the recorded reference spectrum for citric acid (Fig. 1b) and on the spectra of several known decomposition intermediates of citric acid, namely trans-aconitic, itaconic and citraconic acid as well as itaconic and citraconic anhydride, which are reported earlier [40,45].

In Fig. 3, water ( $m/z = 18$ ) is seen at about  $100^\circ C$  (Fig. 3), corresponding to the first weight loss in the TGA profile (Fig. 2a). This is due to the evaporation of residual solvent from the sample.

The second decomposition region situated at the temperature range around  $200^\circ C$ , consists of several chemical processes, in which the organic gel matrix partly decomposes.  $H_2O^+$ ,  $NH_3^+$ ,

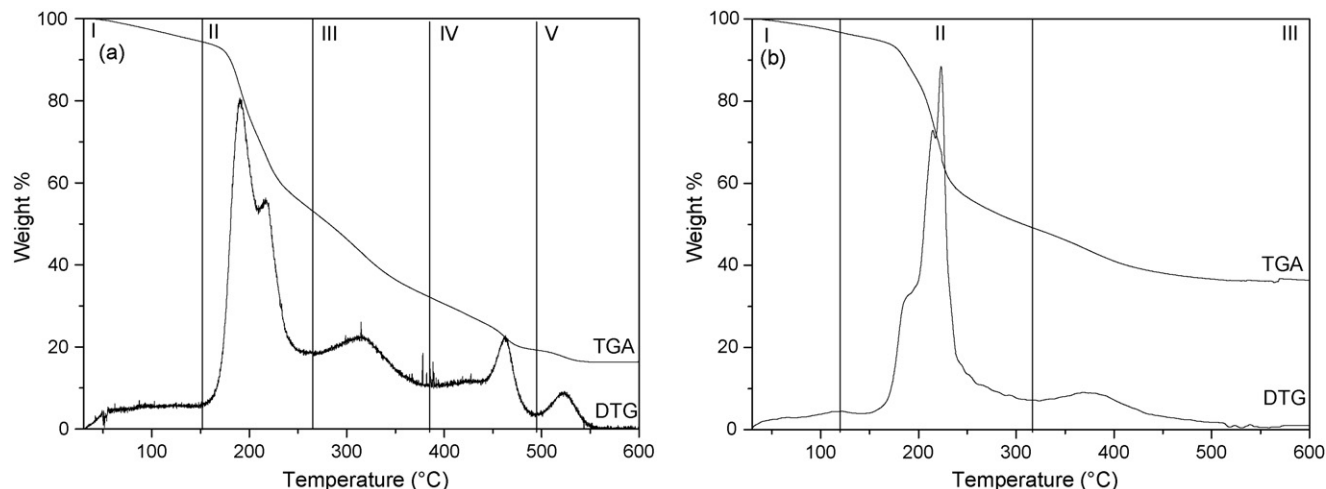


Fig. 2. TGA/DTG for a 0.8 M citratoperoxo-Ti(IV)-gel (25 mg) in (a) dynamic dry air ( $5^\circ C\ min^{-1}$ ) and (b)  $N_2$  ( $5^\circ C\ min^{-1}$ ).

Table 2

Peak assignment and occurrence of mass fragments in TGA-MS of the citratoperoxo-Ti(IV)-gel and the PVA modified citratoperoxo-Ti(IV)-gel in dry air and inert atmosphere

<i>m/z</i>	Fragment(s)	Citratoperoxo-Ti(IV)		PVA modified citratoperoxo-Ti(IV)	
		Peaks in dry air at temperature (°C)	Peaks in N <sub>2</sub> at temperature (°C)	Peaks in dry air at temperature (°C)	Peaks in N <sub>2</sub> at temperature (°C)
17	NH <sub>3</sub> <sup>+</sup>	195; 220; 320; 465; 530	195; 225; 358	190; 220; 310; 465; 480	190; 220; 380
18	H <sub>2</sub> O <sup>+</sup>	100; 195; 215; 310; 460	100; 190; 220; 365	100; 195; 220 (broad); 470	100; 190; 220; 370
30	NO <sup>+</sup>	465; 530		460; 480	
39	C <sub>3</sub> H <sub>3</sub> <sup>+</sup>	195; 225	190; 225	195; 220	200; 225
41	C <sub>2</sub> H <sub>3</sub> N <sup>+</sup> , <sup>13</sup> C <sub>3</sub> H <sub>4</sub> <sup>+</sup>	195; 220; 330; 460; 525	195; 220; 280; 390	180; 210; 300 (broad); 460; 480	195; 225; 300; 380 (broad)
43	CH <sub>3</sub> CO <sup>+</sup>	195; 225; 330; 460; 530	190; 220; 285	190; 220 (broad); 460; 480	195; 220; 310
44	CO <sub>2</sub> <sup>+</sup>	195; 220; 320; 460; 525	190; 220; 275; 385	195-375 (broad); 460; 480	190; 220; 310; 380
45	<sup>12</sup> COOH <sup>+</sup> , <sup>13</sup> COO <sup>+</sup>	195; 225; 315; 460; 525	190; 220; 290; 380	195-375 (broad); 460; 480	190; 220; 310; 380
59	C <sub>2</sub> H <sub>5</sub> NO <sup>+</sup>	195; 225	190; 220; 280	200; 230	200; 220
68	C <sub>4</sub> H <sub>4</sub> O <sup>+</sup>	200; 225	190; 220	210; 230	200; 225

CO<sub>2</sub><sup>+</sup> and the mass fragments *m/z* 15; 30; 41; 43; 59 and 68 are released. The NH<sub>3</sub><sup>+</sup> peak at this temperature can be ascribed to the decomposition of uncomplexed ammonium citrate, formed from the ammonia added and the excess of citric acid present in the Ti(IV)-solution. Other possible decomposition products

of ammonium citrate, which originate by dehydration reactions are amides [46]. An indication for the formation of amides is the release in dry air and in inert atmosphere of a fragment with *m/z* 41, which refers to CH<sub>2</sub>=C=NH<sup>+</sup>. This is a typical ion fragment formed by a McLafferty rearrangement after ionization of an aliphatic nitrile containing a  $\gamma$ -hydrogen [47]. The latter is formed out of an amide by dehydration. Also *m/z* 59 (NH<sub>2</sub>-C(OH)=CH<sub>2</sub>) is a characteristic fragment of a primary amide [47].

Also around 200 °C, water is liberated together with C<sub>3</sub>H<sub>3</sub><sup>+</sup> (*m/z* 39), CH<sub>3</sub>O<sup>+</sup> (*m/z* 43) and C<sub>4</sub>H<sub>4</sub>O<sup>+</sup> (*m/z* 68) (Fig. 3). These mass fragments indicate the decomposition of free citric acid, formed out of ammonium citrate, into unsaturated carboxylic acid and anhydride [40]. The liberation of CO<sub>2</sub> in this temperature region is due to decarboxylation reactions and not to a combustion reaction since it is also seen in inert atmosphere (Fig. 4). These results are in accordance with Rajendran et al. [48] and Van Werde et al. [46]. They report that citric acid decomposes at low heating rates via a series of endothermic dehydroxylation and decarboxylation reactions with formation of successively aconitic acid, itaconic acid, itaconic anhydride and citraconic anhydride.

Around 310 °C the third region in the decomposition pathway of the citratoperoxo-Ti(IV)-gel takes place. The fragments detected with MS in this temperature region are CH<sub>3</sub><sup>+</sup> (*m/z* 15), NH<sub>3</sub><sup>+</sup> (*m/z* 17), H<sub>2</sub>O<sup>+</sup> (*m/z* 18), C<sub>2</sub>H<sub>3</sub>N<sup>+</sup> (*m/z* 41), CH<sub>3</sub>CO<sup>+</sup> (*m/z* 43), CO<sub>2</sub><sup>+</sup> (*m/z* 44), <sup>13</sup>CO<sub>2</sub><sup>+</sup> or COOH<sup>+</sup> (*m/z* 45). These fragments indicate that there are still organic compounds which combust or undergo dehydration and decarboxylation at 310 °C. This is in contrast with the reference citric acid (Fig. 1a) and anhydrides [40], which are fully decomposed at temperatures below 250 °C. Therefore, we can conclude that in the third region decomposition of citrato ligands coordinated to the metal ions takes place. The fact that in the citratoperoxo-Ti(IV)-precursor gel citric acid is coordinated to the Ti<sup>4+</sup> ions is also supported by an FTIR study (Fig. 6a and b) in Section 3.1.2.

NH<sub>3</sub><sup>+</sup> (*m/z* 17), NO<sup>+</sup> (*m/z* 30), H<sub>2</sub>O<sup>+</sup> (*m/z* 18) together with the organic compounds CH<sub>3</sub><sup>+</sup> (*m/z* 15), C<sub>2</sub>H<sub>3</sub>N<sup>+</sup> (*m/z* 41), CH<sub>3</sub>CO<sup>+</sup> (*m/z* 43), CO<sub>2</sub><sup>+</sup> (*m/z* 44), and <sup>13</sup>CO<sub>2</sub><sup>+</sup> or COOH<sup>+</sup> (*m/z* 45) are liberated in the last two decomposition regions, centered

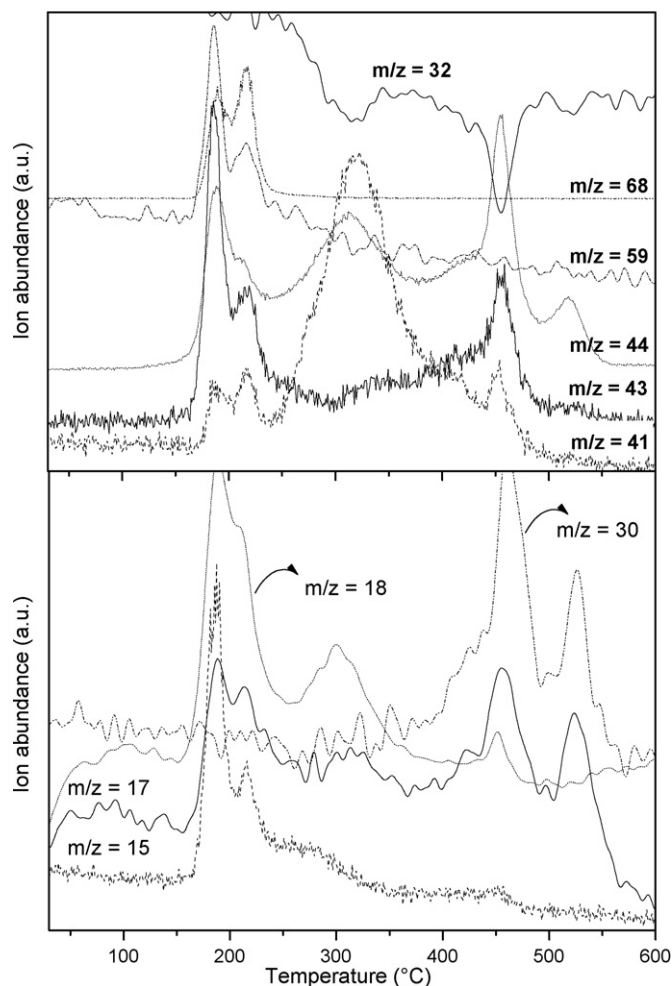


Fig. 3. TGA-MS in dynamic dry air (5 °C min<sup>-1</sup>) for a 0.8 M citratoperoxo-Ti(IV)-gel (25 mg).

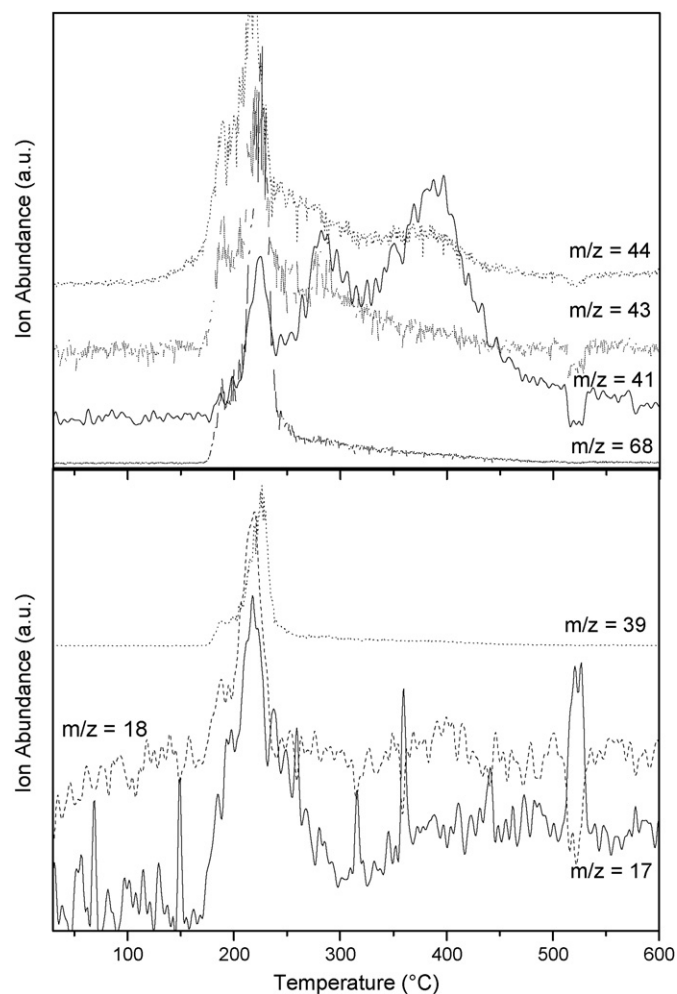


Fig. 4. TGA-MS in  $N_2$  ( $5^\circ C \text{ min}^{-1}$ ) for a 0.8 M citratoperoxo-Ti(IV)-gel (25 mg).

at respectively 460 and 520 °C. During these last steps the residual organic compounds left in the gel are decomposed oxidatively in dry air, resulting in a weight loss of about 16% (Fig. 2a). The consumption of oxygen in the TGA furnace is illustrated by the decrease of the  $m/z$  32 signal ( $O_2^+$ ) in TGA-MS (Fig. 3).

When comparing the MS data recorded in inert atmosphere (Fig. 4) with those in dry air (Fig. 3) it is clear that due to the absence of oxygen the citrato ligands are not burned away. Instead a gradual decomposition of the residual organic matter takes place, which is not fully completed at 600 °C, as seen in the TGA profile (Fig. 2b). In contrast with the sample treated in dry air, which shows a white colour and a weight loss of 83.7%, this sample is coloured black and a weight loss of only 63.7% is obtained.

An XRD spectrum taken after heating the gel in dry air at  $5^\circ C \text{ min}^{-1}$  up to 600 °C, reveals that both the anatase and rutile crystalline phases of titania are present (Fig. 5a).

### 3.1.2. The gel structure

The FTIR spectrum for the citratoperoxo-Ti(IV)-precursor gel dried at 60 °C is shown in Fig. 6a and b. The region between 2300 and 3700  $cm^{-1}$  shows absorption bands which can be

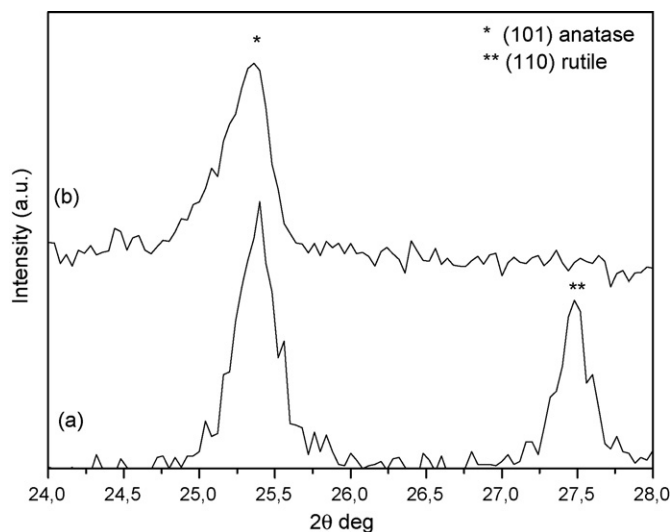


Fig. 5. Powder X-ray diffraction spectra (XRD) of (a) a 0.8 M citratoperoxo-Ti(IV)-gel and (b) a PVA modified 0.8 M citratoperoxo-Ti(IV)-gel, both heated in dynamic dry air up to 600 °C ( $5^\circ C \text{ min}^{-1}$ ).

ascribed to the O–H stretches of the residual  $H_2O$  and carboxylic acids and to the N–H stretches of ammonium. Also the C–H stretching vibrations are situated in this region and originate from the citrates. The broadness of the band is due the fact that a great amount of O–H and N–H functional groups form hydrogen bonds.

The peak at 1720  $cm^{-1}$  can be assigned to the C=O stretch of a carboxylic acid [47]. The occurrence of this band indicates the presence of protonated acid functions of citric acid in the gel due to the excess of citric acid added during the synthesis, due to the pH of precursor gel and due to the evaporation of ammonia out of the  $COO^-NH_4^+$  groups during gelation ( $-COO^-NH_4^+ \rightleftharpoons -COOH + NH_3 \uparrow$ ).

The bands seen at 1599 and 1400  $cm^{-1}$  can be ascribed to respectively the asymmetric and symmetric stretching vibrations of carboxylate functions of citrate ions bound to ammonium groups ( $\nu COO^-NH_4^+$ ) [47]. The occurrence of these ammonium bound carboxylate functions is also seen with MS (see Section 3.1.1). In this way it is proven that, even at this low pH, at least one of the acid functions of the citric acid is deprotonated. When taking a closer look at this band a weak shoulder can be detected at 1565  $cm^{-1}$ . According to Nakamoto et al. [49] this peak results from the asymmetric stretching vibration of  $COO^-Ti^{4+}$ , which indicates the presence of metal bound carboxylate functions. The accompanying symmetric stretching vibration  $\nu_{sym}(COO^-Ti^{4+})$  appears at 1400  $cm^{-1}$ . Consequently, the  $\Delta$  value [ $\nu_{as}(COO^-) - \nu_s(COO^-)$ ] is 165  $cm^{-1}$ , indicating a bridging interaction between a carboxylate ion and two  $Ti^{4+}$  ions. However, the absorption band around 1600  $cm^{-1}$  also shows a weak shoulder at 1635  $cm^{-1}$ , which results in a  $\Delta(\nu_{as} - \nu_{sym})$  of 235  $cm^{-1}$ , pointing to a unidentate carboxylate coordination [48]. Considering the broadness of the band around 1600  $cm^{-1}$ , it is very difficult to draw conclusions concerning the coordination of the carboxylate groups to the metal ions. However, since citrate ions are bound to the  $Ti^{4+}$  ions we may conclude that citrato-Ti(IV)-complexes are present in the

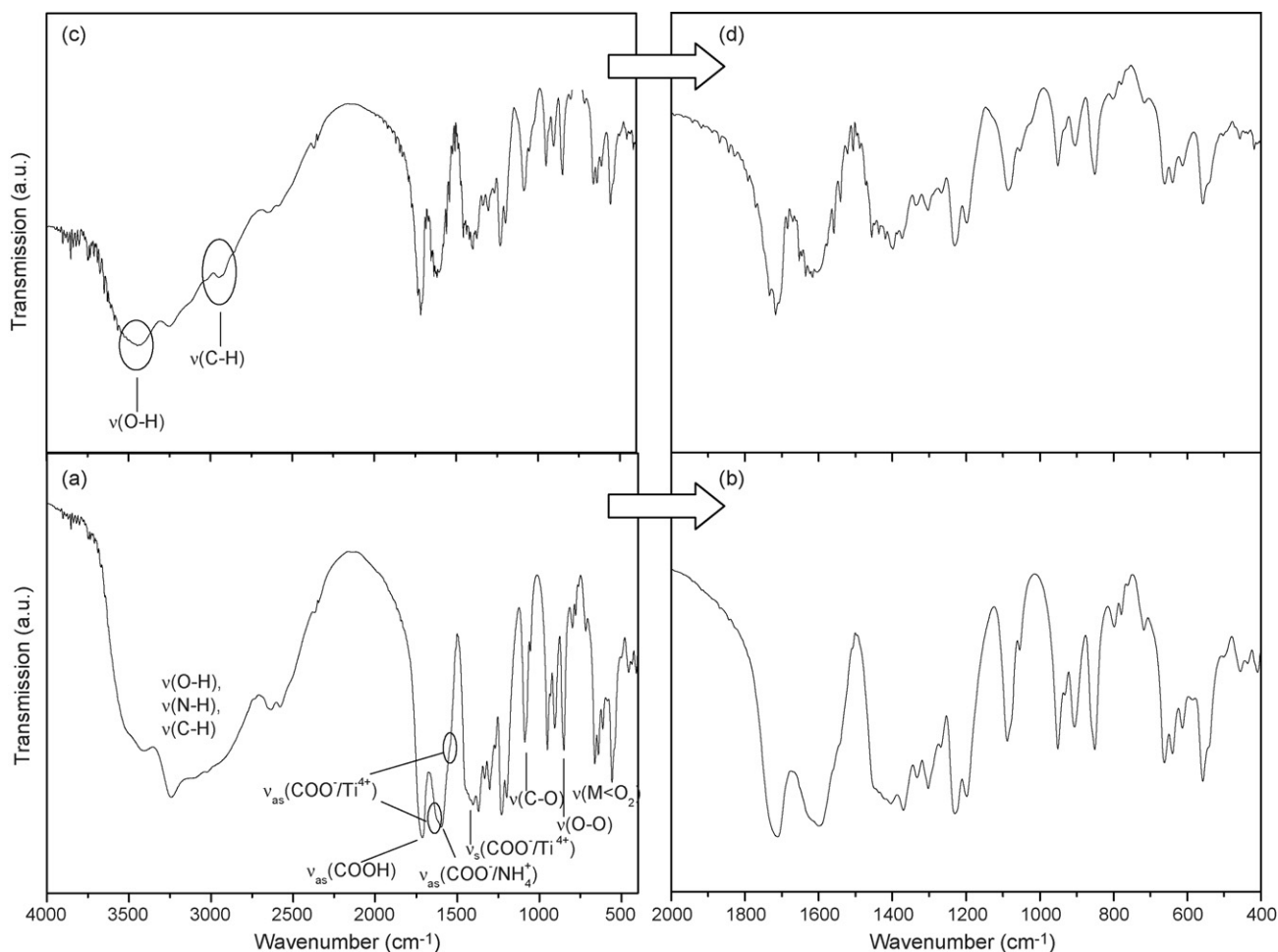


Fig. 6. FTIR spectra and details of the FTIR spectra ( $2000\text{--}400\text{ cm}^{-1}$ ) of (a, b) a 0.8 M citratoperoxo-Ti(IV)-gel dried at  $60\text{ }^{\circ}\text{C}$ ; (c, d) a PVA modified 0.8 M citratoperoxo-Ti(IV)-gel dried at  $60\text{ }^{\circ}\text{C}$ .

precursor gel. This is also confirmed by a strong vibration at  $1088\text{ cm}^{-1}$ , which can be assigned to the C–O stretch of a  $\alpha$ -hydroxy group of citric acid coordinated to the metal ion [50].

The intense absorption band at  $860\text{ cm}^{-1}$  points to ‘side-on’ bidentate peroxy-groups. The O–O stretch in free hydrogen peroxide is seen at  $877\text{ cm}^{-1}$ . The shift of this stretch to a lower wavenumber is due to the complexation of the peroxy-groups to the  $\text{Ti}^{4+}$  ions. The strong bands in the wavenumber region of  $500$  to  $700\text{ cm}^{-1}$  are likely to arise from the symmetric and asymmetric peroxy-Ti stretching vibrations [51]. In this way, it is confirmed that at pH 2.0 peroxy groups are coordinated to the metal ion. This is also seen by Mühlebach et al. as well [52]. They also report that terdentate ligands are well suited to chelate peroxotitanium. This is confirmed in this study by the use of citric acid, which also is a terdentate ligand.

To summarize, from the complementary TG-MS and FTIR data it can be concluded that, even at an acidic pH ( $\text{pH}=2.0$ ),  $\text{Ti}^{4+}$  ions in the precursor gel are encapsulated in a citratoperoxo-complex. This is in accordance with Kakihana et al. [43]. They report that water-based solutions of the tetranuclear complex  $(\text{NH}_4)_8[\text{Ti}_4(\text{C}_6\text{H}_4\text{O}_7)_4(\text{O}_2)_4]\cdot 8\text{H}_2\text{O}$  are stable over a broad range of pH values ( $\text{pH} 1\text{--}14$ ). Also a mononuclear Ti(IV)-citrate complex [53] and a dinuclear Ti(IV)-peroxy-citrate complex

[54] crystallized from aqueous solutions at specified pH values are described in literature.

However, based on the above results the detailed structure of the complex in the precursor gel at pH 2.0 cannot be deduced.

### 3.2. PVA-modified citratoperoxo-Ti(IV)-precursor gel

#### 3.2.1. Thermal decomposition

The TGA and DTG data of the PVA modified 0.8 M citratoperoxo-Ti(IV)-precursor gel, measured at a heating rate of  $5\text{ }^{\circ}\text{C min}^{-1}$  in dry air and inert atmosphere ( $\text{N}_2$ ) are shown in respectively Fig. 7a and b. As a reference polyvinylalcohol is heated in dry air ( $100\text{ ml min}^{-1}$ ) in the TGA at the same heating rate as the citratoperoxo-Ti(IV)-gels ( $5\text{ }^{\circ}\text{C min}^{-1}$ ) (Fig. 7c).

By comparison of Fig. 7a and b with Fig. 2a and b, respectively, we can conclude that the decomposition pathways of the PVA modified 0.8 M citratoperoxo-Ti(IV)-precursor gel in dry air and nitrogen are similar to the decomposition pathways of the citratoperoxo-Ti(IV)-precursor without PVA. However, for the decomposition of the PVA modified precursor gel in dry air, the peaks occurring from the mass losses in step 4 and 5 are not very well separated. Moreover, compared with the decomposition of the Ti(IV)-precursor gel without PVA in dry air, the last

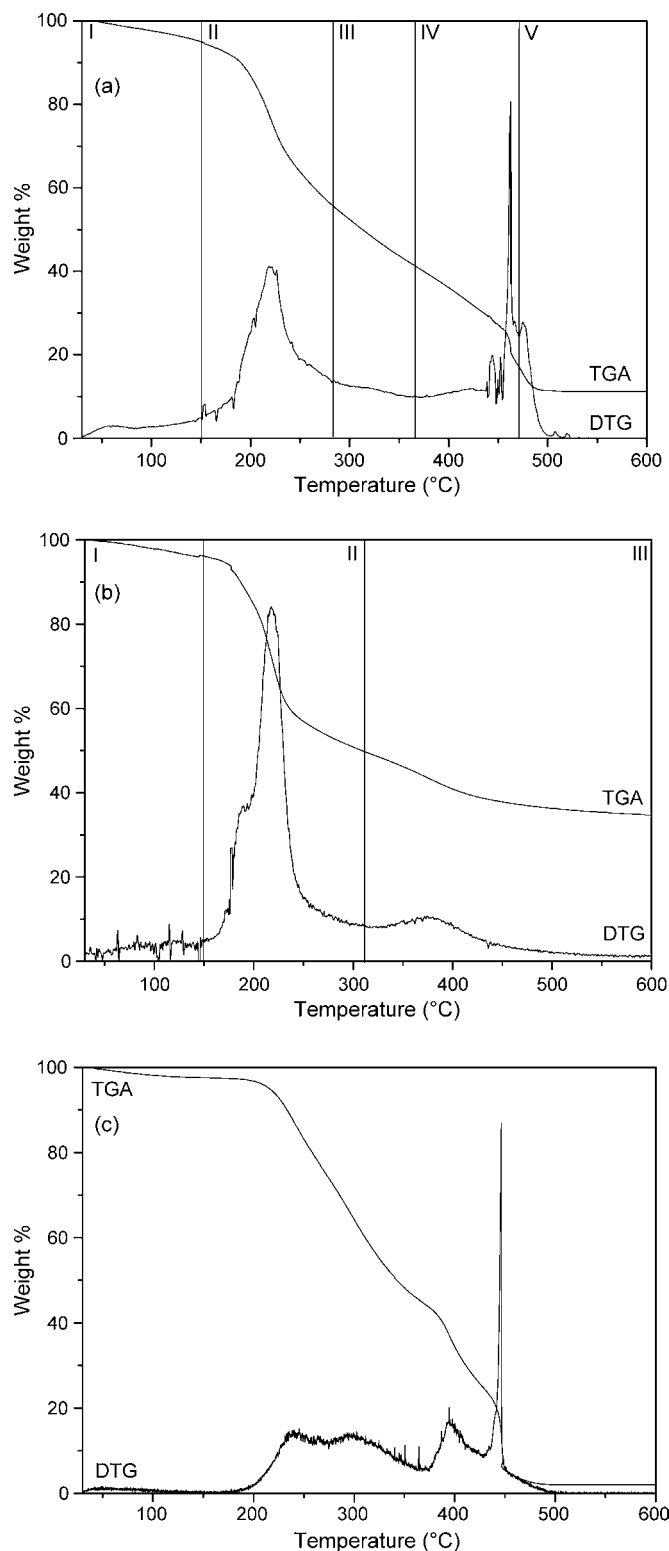


Fig. 7. TGA/DTG for a PVA modified 0.8 M citratoperoxo-Ti(IV)-gel (25 mg) in (a) dynamic dry air (5 °C min<sup>-1</sup>) and (b) N<sub>2</sub> (5 °C min<sup>-1</sup>), (c) PVA (25 mg) in dynamic dry air (5 °C min<sup>-1</sup>).

step shows a 50 °C shift to a lower temperature. The additional peak seen at 445 °C can be assigned to the decomposition of polyvinyl alcohol, present in the precursor gel. This is confirmed by de TGA/DTG data of PVA, shown in Fig. 7c.

We can conclude that also in this precursor citrato ligands are coordinated to the metal ions, because if citric acid was not coordinated we would expect total decomposition at a much lower temperature. The interpretation of the MS data (Figs. 8 and 9) is analogue to Section 3.1.1.

An XRD spectrum taken after heating the gel in dry air at 5 °C min<sup>-1</sup> up to 600 °C, reveals that only the anatase crystalline phases of titania is present (Fig. 5b). This is in contrast with the phase composition of a citratoperoxo-Ti(IV)-precursor gel without PVA and crystallized at 600 °C. XRD-data (Fig. 5a) of the latter illustrate that both the anatase and rutile crystalline phase are present. These results indicate the influence of polyvinyl alcohol on the phase formation.

### 3.2.2. The gel structure and composition of the solid phase

The FTIR spectrum of the PVA modified 0.8 M citratoperoxo-Ti(IV)-precursor gel dried at 60 °C is shown in Fig. 6c and d. The IR spectrum is nearly identical to the one recorded for the original citratoperoxo-Ti(IV)-precursor gel (see Section 3.1.2),

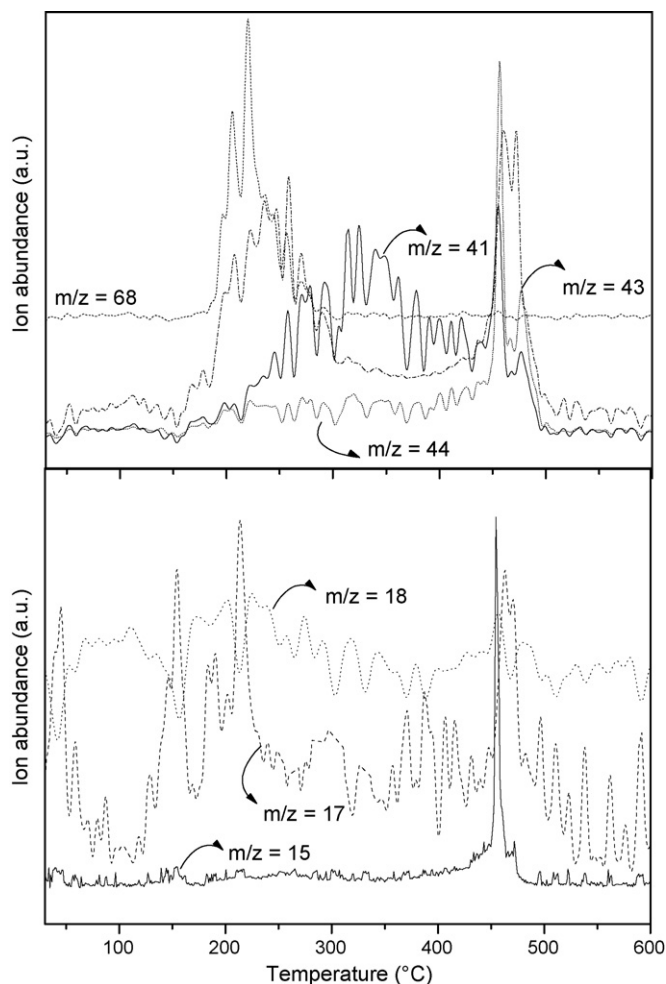


Fig. 8. TGA-MS in dynamic dry air (5 °C min<sup>-1</sup>) for a PVA modified 0.8 M citratoperoxo-Ti(IV)-gel (25 mg).

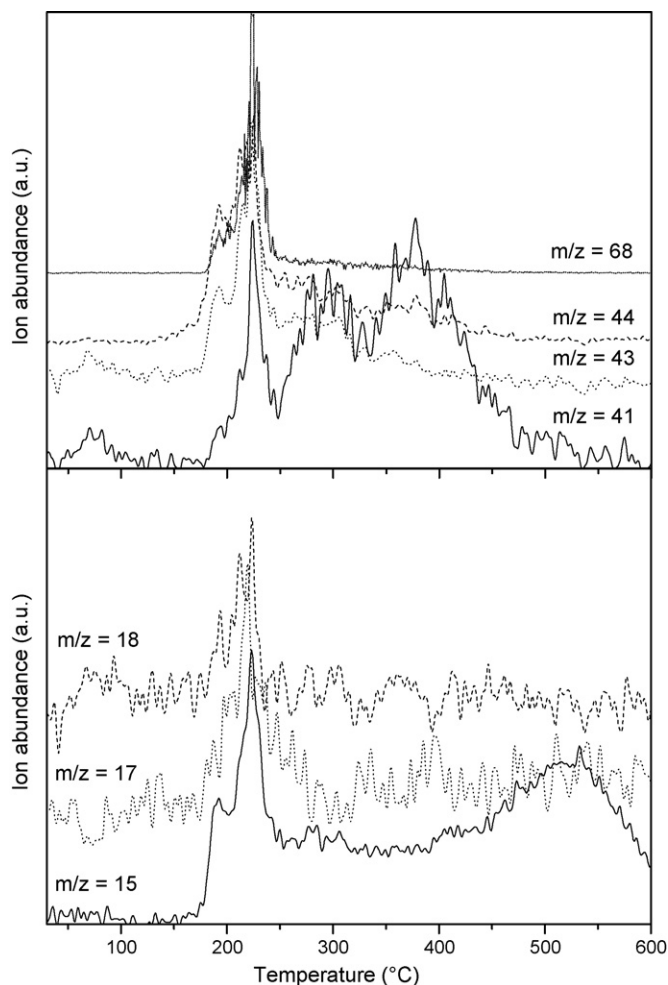


Fig. 9. TGA-MS in  $N_2$  ( $5^\circ C \text{ min}^{-1}$ ) for a PVA modified 0.8 M citratoperoxo-Ti(IV)-gel (25 mg).

confirming the conclusion drawn from the TGA-MS data that even in the presence of polyvinyl alcohol citratoperoxo-Ti(IV)-complexes are present in the precursor solution. However, small differences can be seen between the spectra. Comparing with the original precursor gel, here, a more intense absorption peak is seen at  $3438 \text{ cm}^{-1}$  ( $\nu(\text{O-H})$ ). This can be assigned to the presence of a larger amount of hydroxyl functions coming from polyvinyl alcohol. According to the NIST IR spectrum of polyvinylalcohol [55], the C-H groups give rise to an intense stretching vibration at  $2920 \text{ cm}^{-1}$ .

The FTIR spectra for the PVA modified citratoperoxo-Ti(IV)-gel, recorded after heat treatment at different temperatures, are shown in Fig. 10. The C-O stretch at  $1080 \text{ cm}^{-1}$  has diminished at  $220^\circ \text{C}$  and is absent at  $300^\circ \text{C}$ . At this temperature also the intensity of the  $1565$  and  $1400 \text{ cm}^{-1}$  carboxylate bands is less. This indicates the decomposition of the citrato ligands complexed to the metal ions.

The sample treated at  $300^\circ \text{C}$  also shows two very small peaks at  $1765$  and  $1840 \text{ cm}^{-1}$ . These peaks can be attributed to cyclic anhydrides formed during the decomposition of citric acid.

The small band at  $2215 \text{ cm}^{-1}$  appearing in the spectra at  $450$  and  $550^\circ \text{C}$  can possibly be assigned to the

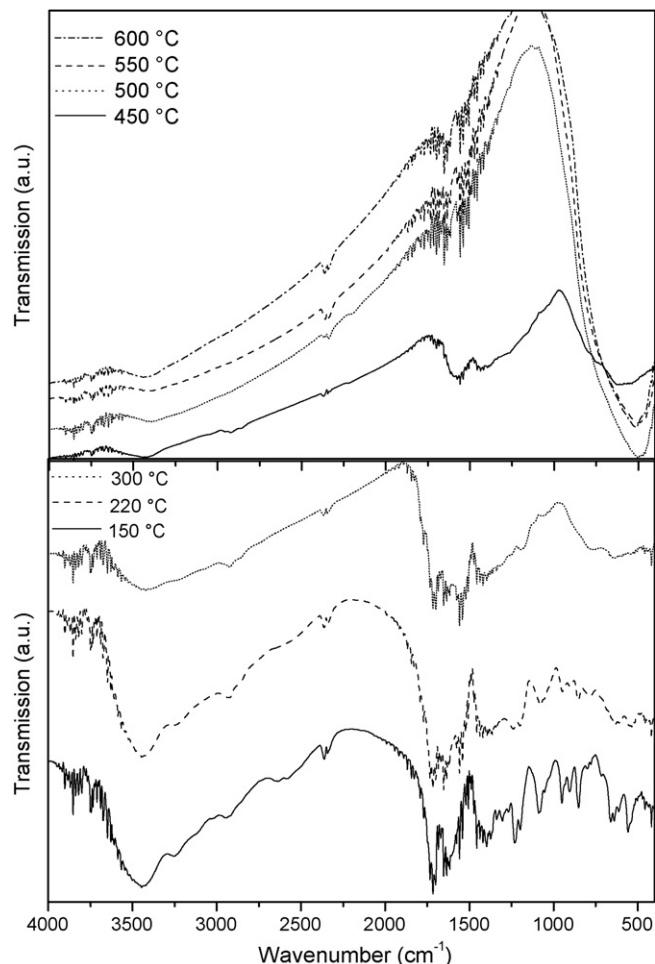


Fig. 10. FTIR spectra of a PVA modified 0.8 M citratoperoxo-Ti(IV)-gel heat treated at the following temperatures:  $150$ ,  $220$ ,  $300$ ,  $450$ ,  $500$ ,  $550$  and  $600^\circ \text{C}$ .

adsorbed carbon monoxide which is liberated at these temperatures.

The intense absorption band at  $860 \text{ cm}^{-1}$ , which points to 'side-on' bidentate peroxy-groups, and the O-O stretching vibrations in the wavenumber region between  $900$  and  $950 \text{ cm}^{-1}$  is smaller around  $220^\circ \text{C}$ , indicating the decomposition of the peroxide coordination.

In the region below  $1000 \text{ cm}^{-1}$  Ti-O stretching vibrations appear in the sample treated at  $300^\circ \text{C}$  [51]. They become stronger at higher temperatures.

The gel, calcined at  $450^\circ \text{C}$ , shows a black colour after thermal treatment, indicating that it still contains some residual organic matter. This is supported by the FTIR spectrum of the sample calcined at this temperature. The three peaks at respectively  $2920$ ,  $1580$  and  $1449 \text{ cm}^{-1}$  demonstrate that still some PVA remains at  $450^\circ \text{C}$ . This is in accordance with the TGA-DTG data of PVA, which show that a complete decomposition of the polymer is only obtained at  $500^\circ \text{C}$  (Fig. 7c). The broad band in the wavenumber region of  $400$  to  $1000 \text{ cm}^{-1}$  is ascribed to Ti-O stretching vibrations [46]. It is confirmed by XRD, that  $\text{TiO}_2$  is formed at  $450^\circ \text{C}$  (data not shown).

At calcination temperatures equal to or higher than  $500^\circ \text{C}$ , the broad band below  $1000 \text{ cm}^{-1}$ , due to Ti-O stretching, is much

more intense. The small peak at  $1620\text{ cm}^{-1}$  in the spectra at 500, 550 and  $600\text{ }^{\circ}\text{C}$  is likely to arise from a deformation vibration of water (artefact). The small peaks at  $2364$  and  $2343\text{ cm}^{-1}$  are artefacts due to the presence of  $\text{CO}_2$  in the apparatus.

To summarize, at calcination temperatures equal to or higher than  $500\text{ }^{\circ}\text{C}$  the organic matrix is fully removed and only  $\text{TiO}_2$  is present in the sample.

#### 4. Conclusion

Both a citratoperoxo-Ti(IV)-gel and a PVA modified citratoperoxo-Ti(IV)-gel at pH 2.0, prepared via an aqueous solution-gel method, are thermally decomposed in dry air and in inert atmosphere. On-line analysis of the evolved gases and FTIR measurements carried out on the solids reveal that in both precursor solutions  $\text{Ti}^{4+}$  ions are encapsulated in a citratoperoxo-Ti(IV)-complex. It is seen that the low pH value (pH=2) of the precursor solution and/or the presence of polyvinyl alcohol in the precursor solution does not affect the formation of citratoperoxo-Ti(IV)-complexes.

In this study, we have also gained insight in the behaviour of both precursor gels during thermal treatment, which is very interesting to determine an optimal heat treatment for thin and thick films deposited out of these precursor solutions. Both the original and PVA modified gel decompose by the same decomposition pathway. In dry air and with a heating rate of  $5\text{ }^{\circ}\text{C min}^{-1}$  this pathway consists of five regions. After evaporation of the remaining solvent at about  $100\text{ }^{\circ}\text{C}$ , decomposition of ammonium citrate occurs. Citrate ligands coordinated to the metal ions decompose in a third step. Finally, in the last two regions the residual organic matter formed during the decomposition process is combusted. Oxygen plays an important role in these last two regions. In inert atmosphere decomposition runs parallel to the one in dry air in the low temperature region. However, from a temperature of approximately  $300\text{ }^{\circ}\text{C}$  onwards the decomposition pathways diverge. Only in dry air it is possible to obtain a full removal of the organic matrix in both gels at temperatures below  $600\text{ }^{\circ}\text{C}$ .

#### Acknowledgements

M.K. Van Bael and A. Hardy are post-doctoral fellows of the Research Foundation Flanders, Belgium (FWO Vlaanderen). The authors would like to thank I. Haeldermans for performing the XRD measurements.

#### References

- [1] O. Carp, C.L. Huisman, A. Reller, *Prog. Solid State Chem.* 32 (2004) 33–177.
- [2] M. Grätzel, *J. Sol–Gel Sci. Technol.* 22 (2001) 7–13.
- [3] M. Grätzel, *J. Photochem. Photobiol. A: Chem.* 164 (2004) 3–14.
- [4] C.G. Granqvist, *Adv. Mater* 15 (2003) 1789–1803.
- [5] L.R. Skubal, N.K. Meshkov, M.C. Vogt, *J. Photochem. Photobiol. A: Chem.* 148 (2002) 103–108.
- [6] A. Fujishima, *J. Photochem. Photobiol. C: Photochem. Rev.* 1 (2000) 1–21.
- [7] T. Kemmitt, N.I. Al-Salim, M. Waterland, V.J. Kennedy, A. Markwitz, *Curr. Appl. Phys.* 4 (2004) 189–192.
- [8] L. Zhao, Y. Yu, L. Song, X. Hu, A. Larbot, *Appl. Surf. Sci.* 239 (2005) 285–291.
- [9] N.P. Mellott, C. Durucan, C.G. Pantano, M. Guglielmi, *Thin Solid Films* 502 (2006) 112–120.
- [10] S.B. Deshpande, H.S. Potdar, Y.B. Kholam, K.R. Patil, R. Pasricha, N.E. Jacob, *Mater. Chem. Phys.* 97 (2006) 207–212.
- [11] T. Alapi, P. Sipos, *Appl. Catal. A: Gen.* 303 (2006) 1–8.
- [12] I. Truijten, M.K. Van Bael, H. Van den Rul, J. D’Haen, J. Mullens, *J. Sol–Gel Sci. Technol.* 47 (2007) 43–48.
- [13] S.Y. Choi, M. Mamak, N. Coombs, N. Chopra, G.A. Ozin, *Adv. Funct. Mater.* 14 (2004) 335–344.
- [14] Y. Djaoued, S. Badilescu, P.V. Ashrit, *J. Sol–Gel Sci. Technol.* 24 (2002) 247–254.
- [15] I. Truijten, M.K. Van Bael, H. Van den Rul, J. D’Haen, J. Mullens, Preparation of nanocrystalline titania films with different porosity by water based chemical solution deposition, submitted for publication.
- [16] R. Hill, *J. Non-Cryst. Solids* 218 (1997) 54–57.
- [17] D. Mardare, P. Hones, *Mater. Sci. Eng. B: Solid State Mater. Adv. Technol.* 68 (1999) 42–47.
- [18] M. Yamagishi, S. Kuriki, P.K. Song, Y. Shigesato, *Thin Solid Films* 442 (2003) 227–231.
- [19] J. Boudaden, R.S.C. Ho, P. Oelhafen, H. Schüler, C. Roecker, J.L. Scartezzini, *Sol. Energy Mater. Sol. Cells* 84 (2004) 225–239.
- [20] D. Mardare, C. Baban, R. Gavrila, M. Modeanu, G.I. Rusu, *Surf. Sci.* 507 (2002) 468–472.
- [21] B. Karunakaran, K. Kim, D. Mangalany, J. Yi, S. Velumani, *Sol. Energy Mater. Sol. Cells* 88 (2005) 199–208.
- [22] A. Mills, N. Elliott, I.P. Parkin, S.A. O’Neill, R.J. Clark, *J. Photochem. Photobiol. A: Chem.* 151 (2002) 171–179.
- [23] M. Kang, J.H. Lee, S.H. Lee, C.H. Chung, K.J. Yoon, K. Ogino, S. Miyato, S.J. Choung, *J. Mol. Catal. A: Chem.* 193 (2003) 273–283.
- [24] C.K. Jung, S.B. Lee, J.H. Boo, S.J. Ku, K.S. Yu, J.W. Lee, *Surf. Coat. Technol.* 174–175 (2003) 296–302.
- [25] U. Backman, A. Auvinen, J.K. Jokiniemi, *Surf. Coat. Technol.* 192 (2005) 81–87.
- [26] G.L. Zhao, Q. Tian, Q. Liu, G. Han, *Surf. Coat. Technol.* 198 (2005) 55–58.
- [27] H. Hirashima, H. Imai, M.Y. Miah, I.M. Bountseva, I.N. Beckman, V. Balek, *J. Non-Cryst. Solids* 350 (2004) 266–270.
- [28] N. Kitazawa, K. Sakaguchi, M. Aono, Y. Watanabe, *J. Mater. Sci.* 38 (2003) 3069–3072.
- [29] K. Cassiers, T. Linssen, M. Mathieu, Y.Q. Bai, H.Y. Zhu, P. Cool, E.F. Vansant, *J. Phys. Chem. B* 108 (2004) 3713–3721.
- [30] H.S. Yun, K. Miyazawa, I. Honma, H. Zhou, M. Kuwabara, *Mater. Sci. Eng. C* 23 (2003) 487–494.
- [31] B. Guo, Z.L. Liu, L. Hong, H. Jiang, J.Y. Lee, *Thin Solid Films* 479 (2005) 310–315.
- [32] T. Miki, K. Nishizawa, K. Suzuki, K. Kato, *J. Mater. Sci.* 39 (2004) 699–701.
- [33] H. Thoms, M. Epple, M. Fröba, J. Wong, A. Reller, *J. Mater. Chem.* 8 (1998) 1447–1451.
- [34] J.Y. Zheng, J.B. Pang, K.Y. Qiu, Y. Wei, *J. Mater. Chem.* 11 (2001) 3367–3372.
- [35] M.K. Van Bael, E. Knaepen, A. Kareiva, I. Schildermans, R. Nouwen, J. D’Haen, M. D’Olielaegeer, C. Quaeysaegens, D. Franco, J. Yperman, J. Mullens, L.C. Van Poucke, *Supercond. Sci. Technol.* 11 (1998) 82–87.
- [36] K. Van Werde, G. Vanhoyland, D. Nelis, D. Mondelaers, M.K. Van Bael, J. Mullens, L.C. Van Poucke, *J. Mater. Chem.* 11 (2001) 1192–1197.
- [37] D. Nelis, K. Van Werde, D. Mondelaers, G. Vanhoyland, M.K. Van Bael, J. Mullens, L.C. Van Poucke, *J. Eur. Ceram. Soc.* 21 (2001) 2047–2049.
- [38] A. Hardy, D. Mondelaers, M.K. Van Bael, J. Mullens, L.C. Van Poucke, *J. Eur. Ceram. Soc.* 24 (2004) 905–909.
- [39] J. Pagnaer, A. Hardy, D. Mondelaers, G. Vanhoyland, J. D’Haen, M.K. Van Bael, H. Van den Rul, J. Mullens, L.C. Van Poucke, *Mater. Sci. Eng. B* 118 (2005) 79–83.
- [40] A. Hardy, K. Van Werde, G. Vanhoyland, M.K. Van Bael, J. Mullens, L.C. Van Poucke, *Thermochim. Acta* 397 (2003) 143–153.
- [41] A. Hardy, Ph.D thesis, Limburgs Universitair Centrum, Diepenbeek, 2004.
- [42] A. Hardy et al., manuscript in preparation.

- [43] M. Kakihana, M. Tada, M. Shiro, V. Petrykin, M. Osada, Y. Nakamura, *Inorg. Chem.* 40 (2001) 891–894.
- [44] Thermolab Instruction Manual: Evolved Gas Analyser for Thermal Analysis-Mass Spectrometry, Fisons Instruments, 37.
- [45] J. Fisher, L.H. Merwin, R.A. Nissan, *Appl. Spectrosc.* 49 (1995) 120–126.
- [46] K. Van Werde, D. Mondelaers, G. Vanhoyland, D. Nelis, M.K. Van Bael, J. Mullens, L.C. Van Poucke, B. Van der Veken, H.O. Desseyn, *J. Mater. Sci.* 37 (2002) 81–88.
- [47] T.N. Sorrell, *Interpreting Spectra of Organic Molecules*, University Science Books, California, 1988.
- [48] M. Rajendran, M.S. Rao, *J. Solid State Chem.* 113 (1994) 239–247.
- [49] K. Nakamoto, *Infrared and Raman Spectra of Inorganic and Coordination Compounds, Part B: Applications in Coordination, Organometallic, and Bioinorganic Chemistry*, 5th ed., John Wiley & Sons, New York, 1997.
- [50] N.B. Colthup, L.H. Daly, S.E. Wiberley, *Introduction to Infrared and Raman Spectroscopy*, 3rd ed., Academic Press, San Diego, 1990.
- [51] W.P. Griffith, *J. Chem. Soc.* (1964) 5248–5253.
- [52] J. Mühlebach, K. Müller, G. Schwarzenbach, *Inorg. Chem.* 9 (1970) 2381–2390.
- [53] E.T. Kefalas, P. Panagiotidis, C.P. Raptopoulou, A. Terzis, T. Mavromoustakos, A. Salifoglou, *Inorg. Chem.* 44 (2005) 2596–2605.
- [54] M. Dakanali, E.T. Kefalas, C.P. Raptopoulou, A. Terzis, G.D. Voyiatzis, *Inorg. Chem.* 42 (2003) 4632–4639.
- [55] cited 2006, NIST. [Available online from <http://www.webbook.nist.gov/chemistry/>].